How to quantify factors degrading DNA in the environment and predict degradation for effective sampling design

Thomas Naef, Anne-Laure Besnard, Lisa Lehnen, Eric J. Petit, Jaap van Schaik, Sebastien J Puechmaille

HAL Id: hal-04562561

https://hal.inrae.fr/hal-04562561v1

Submitted on 29 Apr 2024

Environmental DNA
Open Access
Dedicated to the study and use of environmental DNA for basic and applied sciences

WILEY

How to quantify factors degrading DNA in the environment and predict degradation for effective sampling design

Thomas Naef[1] (iD) | Anne-Laure Besnard[2] | Lisa Lehnen[3] (iD) | Eric J. Petit[2] (iD) |
Jaap van Schaik[1] (iD) | Sebastien J. Puechmaille[1,4,5] (iD)

[1]Applied Zoology and Nature Conservation, Zoological Institute and Museum, University of Greifswald, Greifswald, Germany

[2]DECOD (Ecosystem Dynamics and Sustainability), Institut Agro, INRAE, IFREMER, Rennes, France

[3]Senckenberg Biodiversity and Climate Research Center, Frankfurt am Main, Germany

[4]ISEM, University of Montpellier, CNRS, EPHE, IRD, Montpellier, France

[5]Institut Universitaire de France, 75005, Paris, France

Correspondence
Thomas Naef and Sebastien J. Puechmaille, Applied Zoology and Nature Conservation, Zoological Institute and Museum, University of Greifswald, Greifswald, Germany.
Email: thomasnaef.research@gmail.com
and sebastien.puechmaille@umontpellier.fr

Abstract

Extra-organismal DNA (eoDNA) from material left behind by organisms (noninvasive DNA, e.g., feces, hair) or from environmental samples (eDNA, e.g., water, soil) is a valuable source of genetic information. However, the relatively low quality and quantity of eoDNA, which can be further degraded by environmental factors, results in reduced amplification and sequencing success. This is often compensated for through cost- and time-intensive replications of genotyping/sequencing procedures. Therefore, system- and site-specific quantifications of environmental degradation are needed to maximize sampling efficiency (e.g., fewer replicates, shorter sampling durations), and to improve species detection and abundance estimates. Using 10 environmentally diverse bat roosts as a case study, we developed a robust modeling pipeline to quantify the environmental factors degrading eoDNA, predict eoDNA quality, and estimate sampling-site-specific ideal exposure duration. Maximum humidity was the strongest eoDNA-degrading factor, followed by exposure duration and then maximum temperature. We also found a positive effect when hottest days occurred later. The strength of this effect fell between the strength of the effects of exposure duration and maximum temperature. With those predictors and information on sampling period (before or after offspring were born), we reliably predicted mean eoDNA quality per sampling visit at new sites with a mean squared error of 0.0349. Site-specific simulations revealed that reducing exposure duration to 2–8 days could substantially improve eoDNA quality for future sampling. Our pipeline identified high humidity and temperature as strong drivers of eoDNA degradation even in the absence of rain and direct sunlight. Furthermore, we outline the pipeline's utility for other systems and study goals, such as estimating sample age, improving eDNA-based species detection, and increasing the accuracy of abundance estimates.

KEYWORDS
DNA degradation, DNA quality index, environmental DNA, extra-organismal DNA, noninvasive DNA, noninvasive sampling

---

Jaap van Schaik and Sebastien J. Puechmaille shared senior authorship.

404 | **WILEY** Environmental DNA
Open Access
Dedicated to the study and use of environmental DNA for basic and applied sciences

NAEF ET AL.

1 | INTRODUCTION

Genetic material left behind in the environment with direct information about its donor (e.g., feces, hair, feather, and scales), defined as noninvasive DNA (Taberlet et al., 1999), or contained in environmental samples (e.g., water, soil, and sediment), defined as environmental DNA (eDNA) (Thomsen & Willerslev, 2015), is increasingly used in ecological studies and biomonitoring (Lefort et al., 2022; Thomsen & Willerslev, 2015). Despite differences in concentration and sampling approach, DNA from both noninvasive DNA and eDNA starts degrading upon detachment from the organism. Thus, environmental factors influencing DNA degradation are critical for all kinds of extra-organismal DNA (eoDNA; sensu Rodriguez-Ezpeleta et al., 2021), regardless of the invasiveness (Lefort et al., 2022) of the sampling. This is particularly problematic because eoDNA samples often contain low initial quantities of DNA (Taberlet et al., 1999). For noninvasive DNA samples, understanding how environmental factors shape DNA degradation can enable the optimization of sampling protocols to collect samples with less-degraded DNA content, thereby reducing the number of amplification replicates needed to build reliable consensus genotypes (Taberlet et al., 1996). For eDNA studies, variation in the presence/absence or relative abundance or biomass of species across sites or time (Lugg et al., 2017; Rees et al., 2014) can be masked or exacerbated by variation in eDNA degradation (Buxton et al., 2017). Precisely quantifying environmental eoDNA degradation patterns is therefore expected to advance studies addressing various research questions.

Over the last decades, researchers have identified several environmental factors contributing to eoDNA degradation, including humidity, temperature, rainfall, and direct sunlight (Eichmiller et al., 2016; Murphy et al., 2007; Vili et al., 2013). Broadly speaking, DNA degradation rates are highest in warm and humid environments (Vili et al., 2013; Walker et al., 2019), and lowest in dry and cold conditions (Wasser et al., 1997). Longer exposure exacerbates these effects: several studies observed strongly reduced amplification success after only 1–3 days in warm, humid environments (Murphy et al., 2007; Santini et al., 2007). Amplification success also differs with the characteristics of the targeted eoDNA locus (e.g., nuclear vs mitochondrial, sequence/marker lengths) (Broquet et al., 2006) and sample source, and thus needs to be assessed for each specific system.

In this study, we present a novel modeling pipeline comprising seven steps to robustly quantify environmental factors degrading eoDNA and predict site-specific degradation therefrom. We demonstrate its use on feces (here, from bats), the most reported source (48%) of noninvasive DNA sampling (Lefort et al., 2022), to quantify the influence of humidity, temperature, and exposure duration on the amplification success and genotyping errors of eight microsatellite loci and one sex-linked marker. Based on this quantification, we then predict eoDNA degradation at new sites to identify site-specific ideal exposure durations to improve eoDNA quality and sampling efficiency. Lastly, we outline the potential application of the pipeline to systems with other sampling strategies, eoDNA sources, and markers to maximize sampling efficiency, estimate sample age, and improve species detection and abundance estimates from eoDNA.

2 | MATERIALS AND METHODS

2.1 | Sampling

We collected bat droppings at 10 lesser horseshoe bat (*Rhinolophus hipposideros*) maternity roosts in Thuringia (Germany) between 2015 and 2019 (Jan et al., 2019; Lehnen et al., 2021). We sampled each roost twice a year: once in June and once in August, that is, before and after offspring were born. We spread sheets of newspaper under the main hanging sites, and returned after 9–13 days to collect newly deposited droppings (Puechmaille & Petit, 2007). Here, we refer to such a sampling event of 9–13 days within a roost as a "roost-visit" (RV). We only retained the 25 RVs where both roost temperature (°C) and relative humidity (%, hereafter "humidity") were recorded with iButtons (Maxim Integrated Products, 2015) logging every 30–180 min inside the roost. The microclimate of the roosts varied greatly, including hot and dry attics, cold and humid cellars, and natural semi-open caves. We excluded temperature and humidity measures from the first (newspaper deployment) and the last (sample collection) day, because exact deployment and collection times were not always recorded. We stored all droppings of each RV separately in airtight plastic boxes with silica-gel-beads to dry the droppings immediately upon collection (Lehnen et al., 2018). Boxes with samples were kept at room temperature for 1–20 days after collection, and subsequently stored at −20°C prior to extraction to achieve optimal cold and dry storage conditions (Wasser et al., 1997).

2.2 | DNA extraction and genotyping

Following Jan et al. (2019), for the June and August sampling, respectively, we randomly picked 1.1 and 2.1 times as many droppings from the plastic boxes as adults counted in June. To reduce potential contamination, we picked droppings and extracted their DNA at two designated benches in a pre-PCR laboratory (i.e., no PCR products are allowed in the lab) dedicated to *R. hipposideros* noninvasive genetics. We amplified eight microsatellite loci and a sex marker from the extracts in one multiplex, and scored and genotyped them following established laboratory protocols (Zarzoso-Lacoste et al., 2018, 2020). To minimize single-well pipetting errors, we used a multichannel pipette, working strip-wise (eight wells) on 96-well plates. For microsatellite amplification, we loaded three replicates of each sample from the 96-well extraction plates onto three different 384-well PCR plates with a pipetting robot, so that every 384-well PCR plate contained one replicate of a total of four 96-well extraction plates. All further processing was robot-assisted, thereby minimizing well-wise laboratory effects.

We used a multi-tube approach with three replicates to form reliable consensus genotypes. This replicate number is based on Puechmaille et al. (2007) where an average of 2.73 replicates (2.54–3.09, depending on colony) resulted in reliable consensus genotypes for the same species and collection protocol. To be included in a consensus genotype, an allele at a locus had to be present at least twice across the replicates (i.e., two or three out of three). We automated this process using the bioinformatics pipeline described in Zarzoso-Lacoste et al. (2018) and applied by Jan et al. (2019). This pipeline recovers weaker peaks within a replicate due to hierarchical fall back from more stringent peak detection thresholds, while reducing scoring alleles from cross-contamination by combining peak height thresholds, peak height ratios, and a multi-tube approach (Mäck et al., 2021). If more than two alleles were detected at a locus in a replicate, only the highest two were kept, while lower ones, potentially introduced by cross-contamination, were discarded. To avoid scoring a true homozygote locus as a heterozygote locus, second-highest alleles were only accepted at a locus of a replicate if they exceeded a certain height peak ratio compared to the higher peak (see further details in Jan et al., 2019; Zarzoso-Lacoste et al., 2018).

To facilitate comparison to other eoDNA degradation studies, we calculated the commonly used PCR success rate per sample, defined as the proportion of all loci across all replicates that resulted in a scorable peak. However, to measure actual eoDNA degradation, we used the three replicates and the consensus to calculate the more informative quality index (QI) per sample, a measure of locus-wise agreement of single replicates to their consensus genotype (Miquel et al., 2006). QI can range from 0 (indicating amplification failure and/or complete inter-replicate disagreement) to 1 (amplification and agreement of all three replicates with the consensus). If no consensus could be built due to complete failure of amplification in all replicates of that locus, or due to the inability to form an allele-wise majority, the consensus at that locus was scored as NA and the QI as 0.

In the calculation of QI, we deviated from the pipeline of Zarzoso-Lacoste et al. (2018) in two important steps. First, we kept all multi-locus genotypes (MLGs), irrespective of the number of loci with a consensus, to explore the full spectrum of eoDNA degradation in our samples. Second, we skipped the step of manually checking (and eventually correcting) every consensus genotype that differed from others by one or two loci (Puechmaille & Petit, 2007), because we were only interested in measuring eoDNA degradation. Lower QI prior to the manual correction due to disagreement among loci between replicates or inability to form a consensus at a locus can inform about potential degradation of eoDNA (Appendix S1: Supp_01 5), and manual correction would likely weaken such signal. Compared to a manually corrected dataset, only 8.83% of usable samples (>7 consensus loci) in this study would be corrected with a majority (91.7%) being altered at only one consensus locus leading to a theoretical maximum QI deviation of 0.11–0.13 in the few samples distributed over the RVs (Appendix S1: Supp_02). We also removed one locus (RHC108) in 2018 because its consistently low peak height

and amplification failure indicated a laboratory error for that marker in that year (Appendix S1: Supp_03).

2.3 | Statistical analyses

Following protocols proposed by Zuur et al. (2016) and Harrison et al. (2018), we developed an information theory-based frequentist multi-model inference pipeline to quantify and predict degradation of eoDNA, based on environmental factors, in seven steps. Steps 1–3 describe the iterative process of building a final global model fulfilling model assumptions (Figure 1a). In Steps 4–7, we use this final global model to derive all subset models to achieve robust quantification of DNA-degrading factors. We then evaluate their fit, and select one or more best predictive model to inform sampling strategy (Figure 1b).

We split the data from the 25 RVs of the 10 roosts into a model-building and a model-testing dataset. The model-building dataset contained 21 RVs from eight roosts where the logger was placed in the same room or floor where droppings were collected. The test dataset contained four RVs from two roosts where the logger was placed on a different floor (Appendix S1: Supp_04).

We used the generalized linear mixed model (glmm) function of the glmmTMB package (Brooks et al., 2017) for all models. We standardized all continuous predictor variables in the model-building dataset by two standard deviations and centered at zero to correct for differing measuring units and remove correlation between inter-action effects and their main effects (Schielzeth, 2010) and to allow for direct comparison of estimate strengths of continuous and binary categorical predictor within a model (Gelman, 2008). We standardized and centered the test dataset based on the mean and the two standard deviations from above to ensure that the same un-standardized values in both datasets result in the same standardized values without informing the model building about the distribution of the test dataset. All statistical analyses were performed in R 4.1 (R Core Team, 2021) and R Studio 1.4.1717 (RStudio Team, 2021). The complete modeling pipeline, including the raw data table, is available on Dryad as portable R-Project (Naef et al., 2023) to facilitate reproducibility. The structure and comments of the main pipeline R-Script "01_eoDNAQuantificationandSimulation.R" together with the 18 documented custom functions further facilitate the application of our pipeline to other systems.

2.3.1 | Step 1: Formulate global model

We formulated an initial global model to explain eoDNA quality, specified as the binomial response variable QI, composed of nine predictors and one interaction describing temperature, humidity, and exposure duration in our system (Table 1; Figure 1a, Step 1). To describe temperature (T) and humidity (H) curves throughout a RV, we calculated three summary statistics for each: "Max" referring to the maximum recorded value; "Trend" to the median difference in daily

Legend

Datasets

YES Model assumptions fulfilled? NO

Single model   Multiple models

(a) Global model finding process

1. Formulate global model
- eoDNA quality as response (e.g. "QI", "eDNA score")
- Environmental factors + sample age/exposure duration as predictors
- Lab + sampling as random effects
- Select distribution for model

Reformulate global model
Adjust random effects and/or predictors as last resort
(e.g. drop predictor because of multicollinearity)

Independence?
Distribution?

2. Check all model assumptions:
- Outliers
- Dispersion, zero-in/deflation
- Homoscedasticity & uniformity
- Temporal & spatial autocorr.
- Pairwise corr. & multicollinearity (VIF)

NO

3. Automated correction
Calculate all potential corrective models from a combination of reasonable zero-inflation and/or dispersion terms as a separate part of the global model

Keep converging models that fulfill basic model assumptions (VIF<5, correlation<0.6, no. sign. dispersion/zero-inflation)

Select models with best corrective models (ΔBIC<6 or ΔAICc<6)

Cross-validate models to select one corrected global model based on lowest mean squared error (MSE)

NO

YES

YES Final global model

Model building data

(b) Quantification, prediction and simulation

4. Multi-model inference
Build all subsets from **final global model** while keeping random and corrective (zero-inflation and/or dispersion) model structure fixed

Keep converging models fulfilling model assumptions (VIF<5, correlation<0.6, no. sign. dispersion/ zero-inflation)

Cross-validate models and calculate MSE
Select the **top models** within ΔAICc<6

Report single best AICc model estimates
No partial SD standardization
Correct for multiple testing
Calculate marginal effects for this model

One best model?
(AICc weight>0.9)

YES   NO

Standardize model estimates by partial SD
Correct for multiple testing
AICc average those predictors
Calculate multi-model marginal effects of those **top models**

Consider all to select single **best predictive model** (lowest MSE)

5. Evaluate top models
Assess robustness from predictions under cross-validation

Select best single/averaged model predictions (lowest MSE)

6. Test on new data
Assess generalizability by predicting QI on new sites using **best predictive model** (/-combination)

7. Simulate "what if" scenarios to inform sampling
Use the **best predictive model** to simulate ideal exposure duration per sampling site for a desired eoDNA quality
Alternatively, estimate sample age from observed QI

Test data
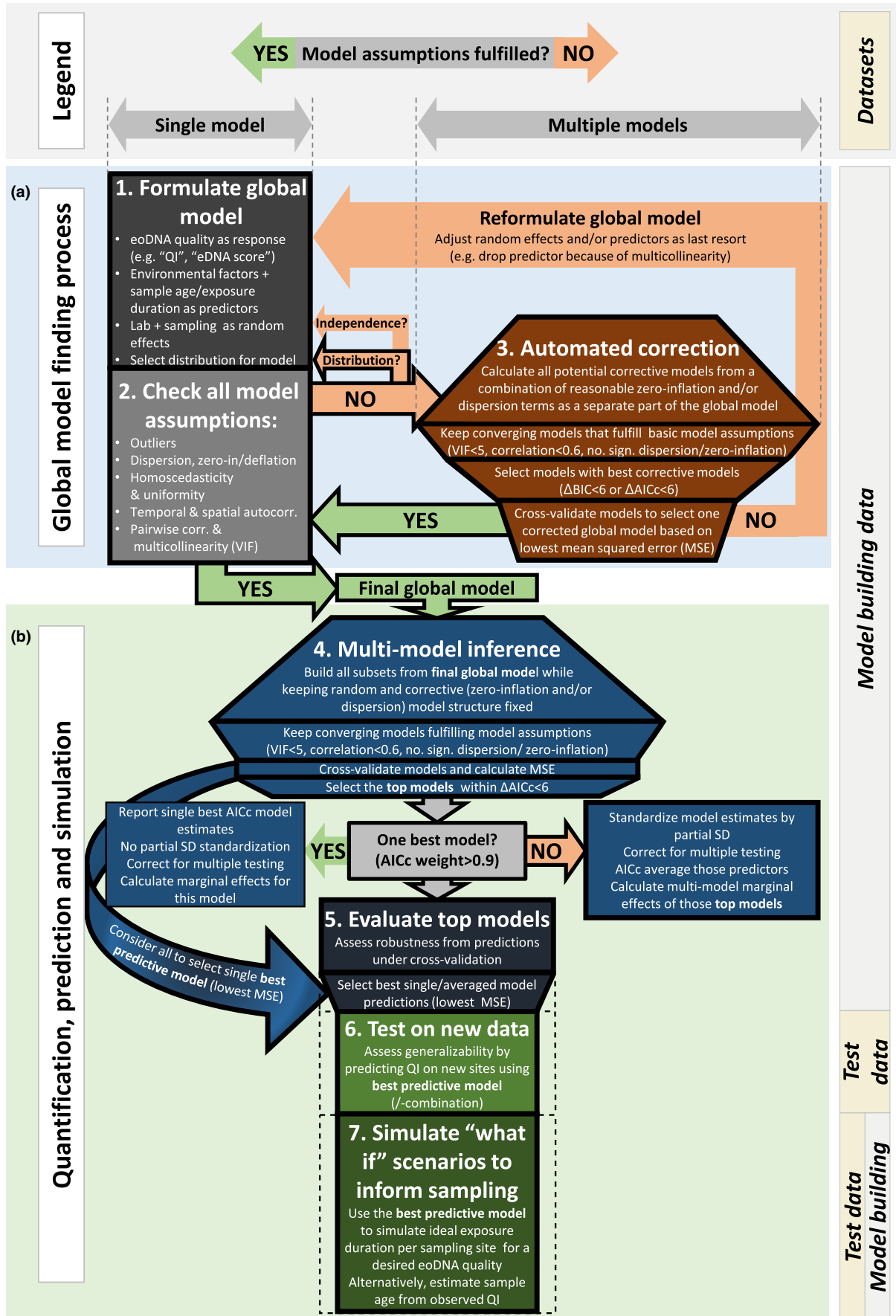**Model building**
Test data
Model building

FIGURE 1 Seven-step-modeling-pipeline to quantify environmental factors degrading extra-organismal DNA and predict site-specific ideal sampling duration (central part), and their involved datasets. (a) Steps 1–3 outline the process to create a final global model that fulfills model assumptions, (b) Steps 4–7 describe the process to generate reliable model estimates and evaluate a predictive model based on the final global model produced in part a. Box width indicates the qualitative number of models involved; a narrowing box indicates a decrease, widening an increase, of the number of models involved per procedure. Folds in cross-validation are generated according to the 21 sampling visits in the model-building dataset. Bold outline indicates the path followed for the case study.

maximum value between two consecutive days; and "HottestDay" and "MoistestDay" referring to the timing of the hottest or moistest day, respectively. The latter were calculated as the day which had the highest median value divided by the total number of sampling days ("Days"). If the first day was the hottest of nine sampled days, for example, the value would be 1/9 (details in Table 1). We added the categorical variable "Sess" (i.e., June or August) to account for potential seasonal effects in eoDNA QI.

We used random intercept terms to control for sampling and laboratory effects. We used "Roost" and "Year" to account for variance introduced by unmeasured site characteristics and annual sampling structure (Table 1). Since we processed droppings per RV, extracts and PCR products were not randomly distributed among extraction and PCR plates. To account for this blocked structure in the laboratory pipeline, we added such blocks of same roost visit samples on same plates ("RVlabunit") as random effects and nested them in their extraction plates ("ExtrPlate"), nested within PCR plates ("PCRPlate"), which were in turn nested within "Year" (Table 1).

2.3.2 | Step 2: Check model assumptions

To ensure unbiased estimates of the fixed effects on QI, we checked the following model assumptions for glmms on this global model (Figure 1). To minimize bias introduced by associations between predictor variables (Dormann et al., 2013), we used the package performance (Lüdecke et al., 2020) to check that multicollinearity did not exceed a variance inflation factor (VIF) of 5 (James et al., 2021) and checked that pairwise correlation between continuous predictor variables were below 0.6 (Freckleton, 2010) using the Hmisc package (Harrell & Charles, 2021). As we detected strong over-dispersion with the residual-based simulation approach of the DHARMa package (Hartig, 2021; Appendix S1: Supp_05 1), we replaced the binomial distribution with a beta-binomial distribution in the global model (Harrison, 2015). Afterward, we still detected violations of model assumptions: three and two predictors exceeded a VIF of 5 and 10, respectively; and severe zero-inflation was observed (5.98 times more zeros observed than simulated with DHARMa, Appendix S1: Supp_06 1-3), leading to Step 3 (automated correction).

2.3.3 | Step 3: Automated correction of violations

To account for these remaining violations, we built and evaluated corrective models using dispersion and zero-inflation modeling (i.e., addition of two separate model formulas in the model in combination

with the conditional formula with its nine predictors) in the glmmTMB package. For the dispersion formula, we included nine predictors likely associated with unexplained dispersion as main effects, and four meaningful interactions (Table 1). For the zero-inflation formula, we used five of the dispersion formula effects and four derived meaningful interactions potentially associated with the creation of additional zeroes (Appendix S1: Supp_07 for the formulas and all predictors involved). To find the best corrective model, we then created all-subset combinations of the specified dispersion and zero-inflation formulas, while maintaining the conditional formula with its nine fixed effects (specified in Step 1). Hereby, we only retained interaction terms if their main effects were present in the corresponding corrective formula. We ignored pairwise correlations of the corrective model, focusing on modeling zeroes and dispersion rather than interpreting single estimates within the corrective model. We calculated 143,417 corrective models, and kept models fulfilling basic model assumptions (VIF < 5, no significant over- or under-dispersion, no significant zero-inflation/deflation) (Appendix S1: Supp_08 1). We then selected the top corrective models within a range of either $\Delta BIC < 6$ or $\Delta AICc < 6$ from the best BIC and AIC model, respectively. We chose both criteria to include overfitting (AICc) and under-fitting (BIC) (Harrison et al., 2018; Appendix S1: Supp_08 2).

To select a single best corrective model, we used blocked cross-validation (abbreviated to just "cross-validation" from here) as a final selection criterion on this subset (Roberts et al., 2017). For cross-validation, we split the data into groups according to the 21 RVs included in the model-building dataset, reflecting our sampling strategy with distinct visits in distinct sites. Then, we excluded one RV and built a model with the remaining 20 RVs. With that model, we then predicted QI for the excluded RV and compared it to the observed QI. This was repeated 21 times until every RV was excluded once. As a measure of the predictive power under cross-validation, we used the mean of the 21 squared errors between observed mean QI and predicted mean QI per RV (MSE). Predictions were always made assuming zero random variance introduced by laboratory and sampling effects, to ensure MSE as most robust and generalizable model selection criterion considering only environmental predictors. We cross-validated all models within $\Delta BIC < 6$ or $\Delta AICc < 6$ from the previous section and selected the single corrective model with the lowest MSE as the final global model (Table 1; Appendix S1: Supp_08 2). Finally, we checked the final global model for outliers, uniformity, homoscedasticity, and independence in the form of temporal (chronologically ordered "Year"/"Sess") and spatial autocorrelation. We detected weak violations in uniformity and homoscedasticity (Appendix S1: Supp_09 1-2), unlikely to affect the overall outcome, as glmms are robust against such violations (Schielzeth et al., 2020) and continued with Step 4.

TABLE 1 Overview of the model-building dataset, including the data type, description, and sample size for each considered variable. Corrective model structure resulted from the automated correction performed in Step 3 of the modeling pipeline. "Z-scored" indicates variable standardization by two standard deviations and centering at 0. Variables of fixed effects and corrective models were always created per roost-visit (RV, 21 values), and are equal for all droppings within the corresponding RV. However, the response variable QI can differ between droppings of the same RV.

Final global model: QI~HMax*TMax+Days+HottestDay+MoistestDay+TTrend+HTrend+Sess			Corrective model	
	Response and fixed effects	Random effects +(1|Roost)+(1|Year/PCRPlate/ExtrPlate/RVLabUnit)	Zero-inflation ~HMin+TMin+AbsHTrend+AbsTTrend	Dispersion ~HMax+AbsTTrend
Model part	Variable (Abbrev.)	Type/transformation	Description and [range of unstandardized variable]	n
Response	Quality Index (QI)	Beta-binomial (logit) (Nsuccess/Nfailure)	Proportion of nuclear replicate loci identical/non-identical compared to consensus locus built over three replicate multi-locus genotypes with nine loci each (eight microsatellites and one sex-linked marker) [3x][0–1]	2309 droppings
Fixed effects	Max. humidity (HMax)	Continuous/Z-scored	Maximum relative humidity [76.8%–100%]	21 values
	Max. temperature (TMax)	Continuous/Z-scored	Maximum temperature [12.6–32.1°C]	21 values
	Temperature trend (TTrend)	Continuous/Z-scored	Trend toward warmer (positive) or colder (negative) days within a single collection period calculated as median of differences between chronologically ordered daily max. temperatures [−0.5°C to 2°C]	21 values
	Humidity trend (HTrend)	Continuous/Z-scored	Trend toward moister (positive) or drier (negative) days within a single collection period calculated as median of differences between chronologically ordered daily max. humidity [−5.1% to +1.4%]	21 values
	Hottest day (HottestDay)	Continuous/Z-scored	Day with max. daily median temperature as proportion of total exposure days [0.18–1]	21 values
	Moistest day (MoistestDay)	Continuous/Z-scored	Day with max. daily median humidity as proportion of total exposure days [0.13–1]	21 values
	Exposure days (Days)	Continuous/Z-scored	Duration of single collection period in a roost in days (maximum possible days a dropping could have been exposed to the environment) [9–13]	21 values
	Session (Sess)	Factor/Reference June	June/August (before/after offspring is born)	2 levels
Random effects	Roost (Roost)	Factor	Different maternity roosts (sampled 21 times from 2015 to 2019)	8 levels
	Year (Year)	Factor	2015–2019	5 levels
	PCR plate (PCRPlate)	Factor	Each PCR plate with 384 wells	30 levels
	Extraction plate (ExtrPlate)	Factor	Each extraction/DNA plate with 96 wells	44 levels
	Roost visit sample block (RVLabUnit)	Factor	Groups of droppings of the same roost visit origin ending up on the same extraction and/or PCR plates (accounting for blocked sample distribution on PCR and extraction plates)	49 levels
Zero-inflation effects	Min. humidity (HMin)	Continuous/Z-scored	Minimum relative humidity [29.3%–100%]	21 values
	Min. temperature (TMin)	Continuous/Z-scored	Minimum temperature [11.0–23.0°C]	21 values
	Absolute humidity trend (AbsHTrend)	Continuous/Z-scored	Measure of absolute variability in max. humidity between days calculated as median of absolute chronological differences of daily maximum humidity [0%–10.9%]	21 values
	Absolute temperature trend (AbsTTrend)	Continuous/Z-scored	Measure of absolute variability in max. temperature between days calculated as median of absolute chronological differences of daily maximum humidity [0 −2°C]	21 values
Dispersion effects	AbsTTrend, HMax	Continuous/Z-scored	Variables already explained in previous rows	21 values

2.3.4 | Step 4: Multi-model inference

The final global model from Step 3 was then used to identify important predictor variables and build a predictive model (Steps 4–7; Figure 1b). First, we created all potential subsets from the final global model, retaining interactions only when the main terms were present. We kept the random effect structure and the corrective model (Table 1) unchanged for all models. As before, only models fulfilling basic model assumptions were retained. We cross-validated all remaining models to calculate MSE. We then selected the top models with $\Delta AICc < 6$, following the recommendation of Harrison et al. (2018) and Richards (2007) (Appendix S1: Supp_10 1). In the absence of one single best model within $\Delta AICc < 6$, defined as AICc weight > 0.9, we averaged all top models (Grueber et al., 2011). Prior to model averaging, we standardized all model coefficients of the top models by their partial standard deviation—a measure combing VIF and standard deviation (Cade, 2015)—to exclude bias arising from different levels of multicollinearity between models containing different predictors. We also adjusted the 95% confidence intervals of estimates for simultaneous hypothesis testing using family-wise correction with the glht function of the multcomp package (Hothorn et al., 2008). We summarized model-averaged marginal effects for all fixed effects of the top models with a custom function based on ggpredict from the ggeffects package (Lüdecke, 2018).

2.3.5 | Step 5: Evaluate top models

We checked overfitting of our top models based on MSE from cross-validation in Step 4. We selected the best predictive model from all cross-validated models in Step 4 with the lowest MSE (Appendix S1: Supp_10 2), including the MSE resulting from combined predictions of the top models, defined as the AICc-averaged predictions under cross-validation. As random effect variance was set to zero for all predictions under cross-validation, predictions could not profit from information from laboratory and field variance. Thus, the best predictive model should also be the most robust and generalizable, depending only on environmental predictors to predict eoDNA degradation as mean QI per RV.

2.3.6 | Step 6: Test on new data

As a final assessment of generalizability of our findings, we tested the predictive power of our best predictive model to predict QI on the test dataset, not used in any of the previous steps. Its four RVs (two new roosts, each sampled twice; Appendix S1: Supp_04) make up 16% of all 25 RVs, which roughly corresponds to the recommended 90% model building and 10% testing data (Zuur et al., 2016). We predicted QI for the test dataset, and calculated the MSE between the mean predicted and observed QI for each RV. In this process, we assumed no additional variance due to laboratory and sampling effects (setting random variance to zero).

2.3.7 | Step 7: Simulate "what if" scenarios to inform sampling

We used the best predictive model in a "what if" scenario (Zuur et al., 2016) to estimate the maximum number of exposure days per roost ("IdealDays") that still yielded a predicted QI of at least 0.95 or 0.99. We reduced the predictor "Days" stepwise by 1 day and slid a window with such reduced length in 1-day steps along the original logged environmental data. For every window, we recalculated the continuous predictors from the logged data to predict its QI. We decreased window length (i.e., "Days") until the median of all same-sized window predictions reached or exceeded the target QI. Those predictions were made assuming no additional variance from random effects. The corresponding final length of "Days" then resulted in "IdealDays" for that RV. To recommend ideal sampling duration per roost, we conservatively selected the minimum "IdealDays" from all assessed RVs from a given roost.

3 | RESULTS

3.1 | eoDNA quality and its environment

For model-building and test dataset combined, QI per sample ranged between 0 and 1 with an average of 0.85. Per RV, the average sample QI varied between 0.59 and 0.98. For better comparison with other eoDNA degradation studies, we also provide the commonly used PCR success rate, ranging from 0 to 1 per sample with an average of 0.9. The average PCR success rate per RV varied between 0.65 and 1 (Appendix S1: Supp_11 2). Environmental variables differed greatly between RVs (Table 1; see Appendix S1: Supp_12 1 for a visual overview).

3.2 | Model building and selection

Of the 143,417 corrective models built in Step 3 to correct for zero-inflation and collinearity issues, only 5892 models converged and fulfilled basic model assumptions. After selecting both the top $\Delta AICc < 6$ and $\Delta BIC < 6$ models, only 104 models remained. Cross-validation of those 104 models resulted in a single best final global model with an MSE of 0.0108 (Appendix S1: Supp_08). This model fulfilled all assumptions, besides negligible deviations from heteroscedasticity and uniformity (Appendix S1: Supp_09 1-2). With this corrective structure for the final global model, we performed multi-model inference (Step 4), resulting in 321 models, which were reduced to 283 after checking model assumptions, and further reduced to 19 top models after selecting for models within $\Delta AICc < 6$ (Appendix S1: Supp_10).

3.3 | Model interpretation

In all 19 top models, we found strong negative effects of maximum humidity ("HMax"), exposure days ("Days"), and temperature

("TMax"), as well as a positive effect of the time when the hottest day occurred ("HottestDay"). Those four effects were consistent in all the 19 top models, even after family-wise correction for simultaneous hypothesis testing (Figure 2).

Between-effect comparisons revealed that "HMax" was the strongest effect, reducing QI 1.42 times stronger than "Days," and 1.82 times stronger than "TMax," according to the AICc-averaged model estimates. The positive effect of "HottestDay" was between the strength of the negative effects "Days" and "TMax," with "HMax" contributing 1.67 times more strongly than "HottestDay." This order ("HMax" > "Days" > "HottestDay" > "T Max") was conserved across single model estimates, and effect strength ratios were similar for all top models. A potential positive effect of "Sess" (higher QI for sampling sessions in August than for June) and a potential negative effect of "HTrend" (trend toward more humid days within a RV) were detected only in 12 and 11 of the 19 models, respectively. These effects vanished after correcting the 95% CI for family-wise multiple testing using glht (Figure 2). "MoistestDay," "TTrend," and "HMax:TMax" did not have a substantial effect, indicated by closely scattered estimates around zero. However, all estimates of "HMax:TMax" were consistently negative, contrary to the other two effects. Estimates and confidence intervals for the six corrective model terms (two dispersion and four zero-inflation, Table 1) were not only highly similar among the 19 top models, but also among all 283 models generated by the multi-model inference that met model assumptions (Appendix S1: Supp_13).

The strong effects of "HMax," "Days," "TMax," and "HottestDay," their order across all 19 top models, and the weak to nonexistent effect of other predictor variables on QI was also confirmed by the slopes and confidence intervals of the fixed marginal effects (Figure 3). The results can be best understood when looking at the extreme values of the environmental variables from the AICc averaged marginal effects: increasing "HMax" from 76.8% to 100% reduced QI from 0.93 to 0.65; increasing "Days" from 8 to 13 days lowered QI from 0.89 to 0.60; and increasing "TMax" from 12.6°C to 32.1°C reduced QI from 0.94 to 0.75. Compared to a QI of 0.76 for the earliest (0.2) "HottestDay," QI was 0.89 for the latest (1.0) "HottestDay."

3.4 | Model evaluation

All 19 top-model predictions of mean QI per RV (Figure 1b, Step 5) came close to their mean observed values (Figure 4), with an AICc-averaged prediction MSE over all RVs of 0.00125, which increased to 0.00849 under cross-validation (Figure 4, squares). The single best predictive model, including only "HMax," "Days," "TMax," "HottestDay," and "Sess" effects (Figure 2, asterisks), could predict mean QI per RV with an MSE of 0.00736 under cross-validation (Figure 4, asterisks). When we applied this best-predictive model to the test dataset (two
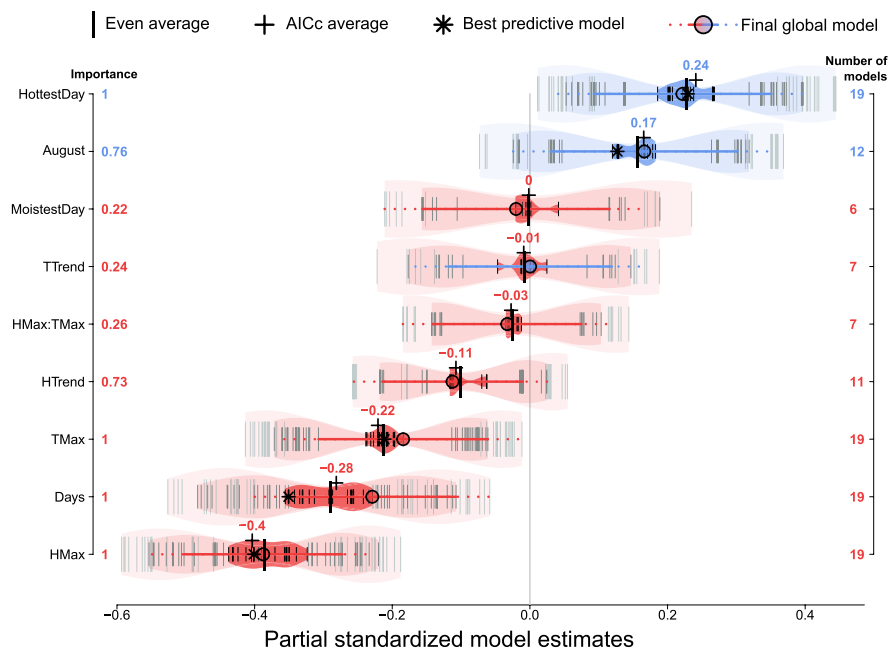

FIGURE 2 Individual effect estimates (darkest shapes and black ticks) and 95% confidence intervals (CI) (lighter shapes and ticks), and their corrected CI for family-wise multiple testing (lightest shapes and ticks) of the 19 top models (ΔAICc < 6). Effect estimates are sorted from negative (red) to positive (blue) by their AICc-weighted average effect estimates (plus symbol, value above). Circles, solid, and dotted horizontal lines indicate the estimates, CIs, and corrected CIs of the final global model also contained within ΔAICc < 6. Best predictive model is the model with lowest mean squared error (MSE) under roost-visit-wise cross-validation without using random effects variance for predictions. Effect estimates are directly comparable within and between models due to standardized input variables (2 SDs) and their predictors (partial SD).

new roosts, four RVs, logging further from some samples) without using the variance introduced by the laboratory and sampling pipeline predictions, errors increased to a MSE of 0.0349 (Figure 4a, asterisk in Test data).

3.5 | Model simulations to inform sampling

The median of the ideal sampling duration over all roosts (Step 7) to achieve a mean QI of 0.95 per roost was 5.5 days, rather than the median of 9 days in our empirical dataset. Roost-specific ideal exposure duration ranged from 2 to 8 days (Figure 4d; Appendix S1: Supp_14). Achieving a mean QI of 0.99 required reducing exposure duration to just 2–3 days, and was only possible in five roosts. In the other three roosts, no amount of reduction could sufficiently increase QI (Appendix S1: Supp_15). We detected an unexpectedly high proportion of droppings with zero QI (11.6%) in RV "Thu21/2017/1," likely due to laboratory effects (Figure 4a, gap between full vs hollow circle). Therefore, we excluded this one roost visit in the calculations for ideal exposure duration for "Thu21."

4 | DISCUSSION

4.1 | Case study

In agreement with the published literature (e.g., Eichmiller et al., 2016; Murphy et al., 2007; Vili et al., 2013; Walker et al., 2019), our model identified the negative effects of high humidity, temperature, and long exposure duration on eoDNA quality. Notably, we also revealed the importance of timing and succession of such environmental conditions, captured by the positive effect of a late occurrence of the hottest day. These effects also remained stable in strength and order among the top models, even after correction for multiple testing, underlining the qualitative and quantitative robustness of our findings. Under cross-validation, when random effect variance was set to zero, QI could still be predicted accurately. However, the model was only able to accurately predict QI for one of the four additional RVs of the test dataset (Figure 4, Test data, gray plus vs. red asterisks). This reduced prediction accuracy in the test dataset was likely because the test dataset did not only introduce completely new sites but also further logger distance. The samples
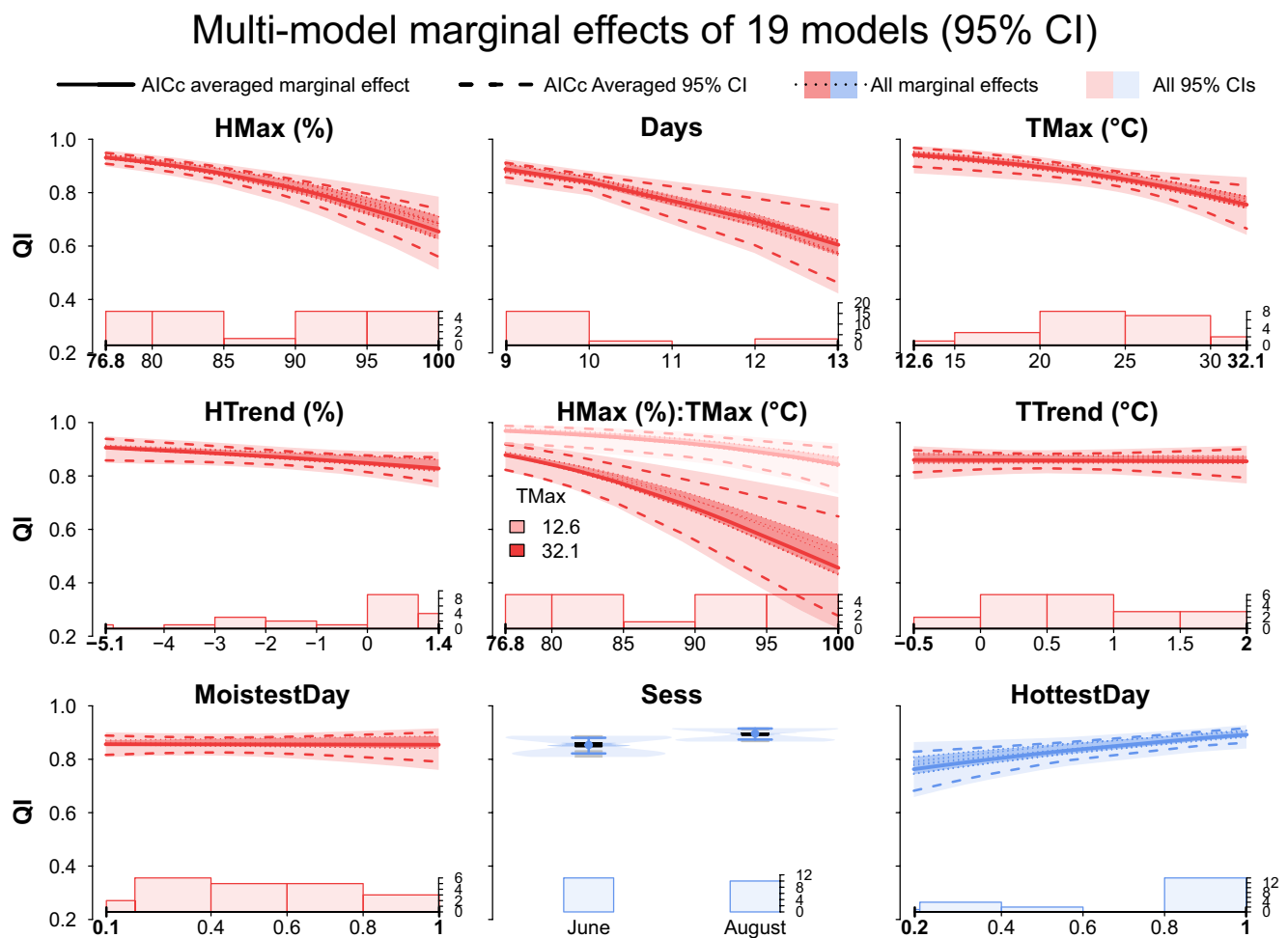

FIGURE 3 Single predicted marginal fixed effects on QI for the 19 top models (ΔAICc < 6) and their AICc averages. The sorted effects from most negative (red) to most positive (blue) are plotted on the same y-scale. Histograms on the x-axis indicate the distribution of the unstandardized predictors with their range in bold over the 21 roost-visits, to assist interpretation of confidence intervals.

were pooled across multiple floors with varying environmental conditions, but only one logger was used to model them while the model-building dataset pooling was restricted to the same room or floor. This likely introduced misrepresentation of logged environmental data for a majority of pooled eoDNA within a RV, potentially reducing prediction accuracy.

While we used abiotic environmental factors to quantify and predict eoDNA degradation, the actual degradation is most likely biotic, caused by free DNAses and microbes in the feces (Dash & Das, 2018; Regnaut et al., 2005). Free DNAses profit from water availability under high humidity and speed up enzymatic processes under higher temperature (Abdel-Gany et al., 2017). Better growth of DNA-degrading microbes at higher temperatures (Eichmiller et al., 2016) further expedites DNA degradation, for example, in feces (Murphy et al., 2007; Nsubuga et al., 2004), feathers (Vili

et al., 2013), and hair (Sawaya et al., 2015). Therefore, temperature and humidity (for terrestrial systems) are good proxies to quantify such biotic processes involved in eoDNA degradation, and as illustrated here can be used to identify optimal sampling strategies based on site-specific (micro-)climatic conditions.

Naturally, increased exposure duration will exacerbate these effects. In our study, the exact exposure duration was unknown for each individual dropping, but we quantified the average environmental effect on all samples from a site. Finally, the positive effect of "HottestDay" (meaning that a later occurrence of the hottest day resulted in less degradation) indicates a potential drying effect on previously humid droppings, also reported for bear hair drying in the sun (Sawaya et al., 2015). We provide further support for the proposed drying effect (Appendix S1: Supp_16–19). It shows that the positive effect does not originate from calculation artifacts of
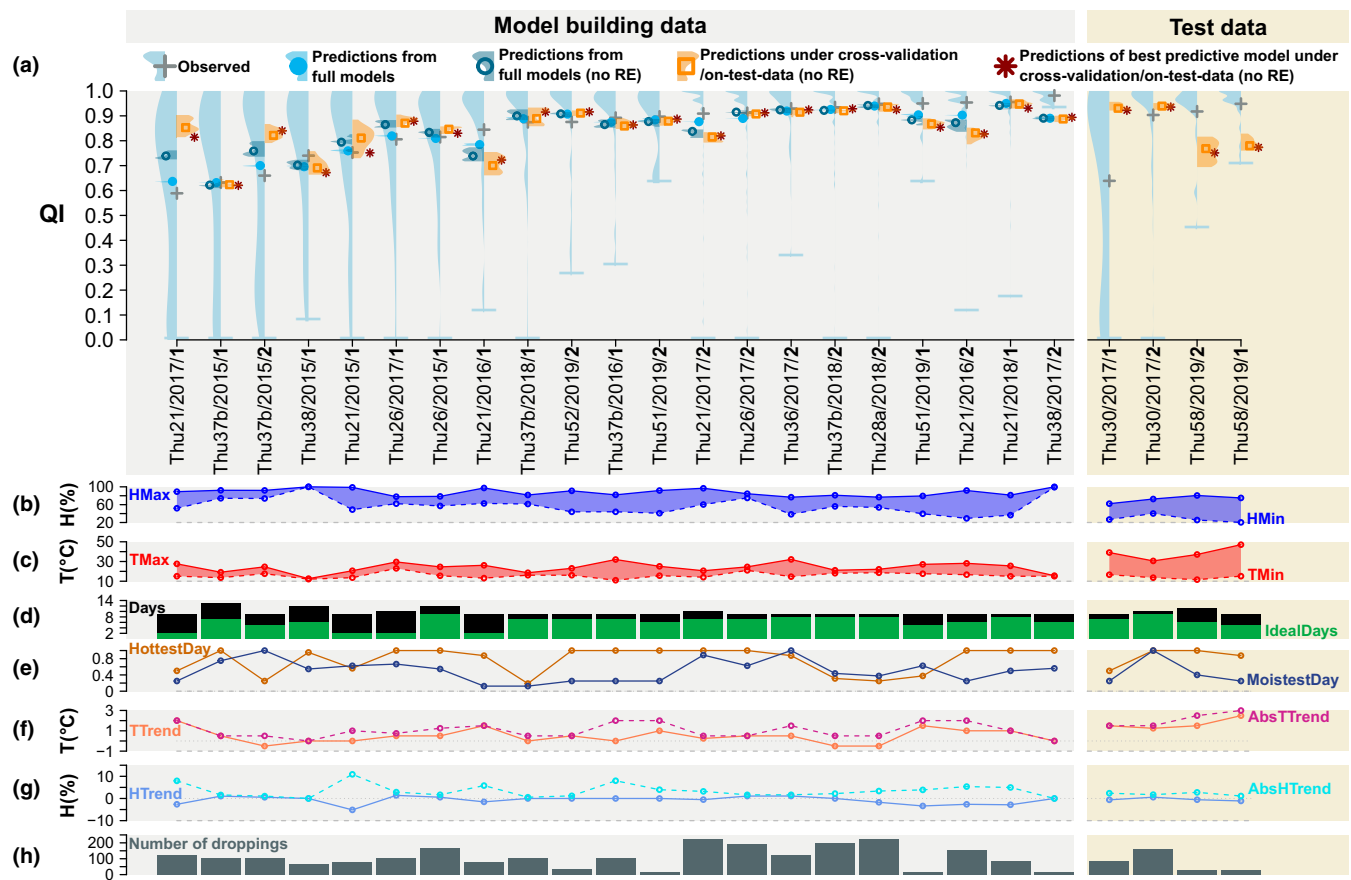

FIGURE 4 Overview of observed QI and environmental conditions and predicted QI based on both the final global model and predictive models for each roost-visit (RV). The 21 RVs used for model building are denoted with a gray background, and the four RVs used as test dataset are on the light brown background. (a) Observed and predicted mean Quality Index (QI) per RV. Names along the x-axis follow the format "Roost"/"Year"/"Sess." RVs are sorted in increasing order according to their mean observed QI (gray plus). Light blue distributions indicate observed QI density (Horizontal ticks indicate the lower limit of the observed QI), medium blue the mean predictions based on the full model, dark blue the predictions based on the full model without using random effect variance (no RE), and orange the predictions based on cross-validation. "Full" indicates predictions are based on the full model-building dataset, unlike in cross-validation, where they are based on the full model-building dataset minus one RV for every RV, Like-colored symbols indicate AICc-averaged predictions of the 19 top models. Red asterisks indicate mean predictions per RV of the best predictive model (lowest mean squared error (MSE) under cross-validation). (b, c, e–g) Unstandardized temperature (reddish) and humidity (bluish) predictors experienced during the duration (d) of a RV used in the models. Solid lines connecting these predictors indicate fixed; dashed lines indicate corrective model predictors. Connections do not imply interpolation. (d) Also shows the estimated ideal sampling duration to reach a QI of 0.95 using the single best predictive model in green. (h) The number of droppings genotyped for each RV.

uninformative "HottestDays" and that the effect only persists when the hottest days occur after humid conditions and when hot afternoons follow humid mornings.

It is important to note that of the nine fixed effects predictors used in our models (Table 1), only sampling session ("Sess," which in our case is imposed by species phenology) and exposure time ("Days") can be easily modified by the surveyor. Particularly, the latter predictor therefore warrants careful consideration when planning eoDNA surveys. As illustrated by our predictive modeling approach, calculating site-specific ideal exposure durations and adapting sampling strategies accordingly can provide valuable insight into how to increase the number of usable genotypes and reduce the need for repeated genotyping.

4.2 | Application of the pipeline to other eoDNA systems

As outlined above, obtaining system and site-specific quantification and predictions for improved sampling efficiency, sample age estimates, species detection, or abundance estimates, will significantly improve and broaden the use of eoDNA. However, performing this task is challenging. Our work proposes a framework and pipeline to perform this task where the user simply needs to adjust specific environmental factors, sample pooling, exposure duration, eoDNA quality, and the sampling and laboratory effects accordingly, as outlined below.

For the predictor variables, measurements of environmental variables affecting eoDNA degradation (e.g., temperature, humidity) are easy to obtain and widely available across the globe (e.g., loggers or weather-stations). Therefore, our pipeline can be applied to many existing datasets. In our study system, the sheltered nature of sites excluded potential effects of rain or direct sunlight. Adding such environmental factors or information on whether samples were collected in sheltered or open locations could further improve predictions, because cover not only protects from rain (Agetsuma-Yanagihara et al., 2017) and sun (Vili et al., 2013) but could also limit drying (Sawaya et al., 2015). The duration of sample exposure (i.e., "sample age") is an important, yet rarely known variable. In our case study, we used maximum possible sample age instead (in the form of exposure time, "Days"). In other systems, maximum possible sample age can be assessed by regular transects to discover new samples, or based on the decrease of the eRNA:eDNA ratio with increasing age (Marshall et al., 2021). Where samples are not clustered in well-defined units like roosts, samples can be pooled within a similar environment (e.g., transect IDs, multiple water samples, building) and according to the closest weather station or data logger. If environmental conditions within a pool vary too much, misrepresentation and therefore lowered accuracy of model estimates and predictions can occur as seen in three out of four RVs in the test dataset (Figure 4a, Test data). When pooled appropriately, the degrading effect of the environment on mean eoDNA quality can be quantified, even when the exact exposure timing is unknown. To capture environmental eoDNA degrading effects and improve predictions, the selection

of different pools should also reflect the variability, range, and combinations of environmental variables within a system, as seen in the RVs of the case study spanning from dry and hot attics to humid and cold basements (Figure 4b–g; Appendix S1: Supp_12).

While we accounted for pairwise correlations and multicollinearity to get unbiased predictors for the quantification (Steps 3–4) in our case study, collinearity can be allowed if predictive models are the only goal and if the underlying correlation is always present and stable in a system (Dormann et al., 2013). Further, predicting ideal sampling duration could also be reversed, estimating sample age from observed QI when environmental conditions are known instead, especially when samples originate from a direct source (e.g., feces, feathers), to ultimately estimate donors' last presence.

Variance introduced by laboratory and sampling procedures should be accounted for with thoughtfully selected random effect structure since it can affect model estimates and prediction accuracy. The latter was demonstrated by the increased MSE when we did not account for variance introduced by random effects (filled vs hollow circles in Figure 4a). Effects of laboratory procedures should not be underestimated, especially when results from different laboratories are compared or combined. We recommend close monitoring of sampling effects and laboratory procedures using high-quality samples (i.e., positive controls). Deviations from the expected high genotype quality can signal the necessity to adapt for sampling and laboratory effects. Plate-wise, robot-assisted work flows further minimize individual laboratory effects, and facilitate their detection and correction because whole plates, rather than individual samples, are affected. As predictive models cannot easily compensate for such effects, the only viable solution when severe laboratory biases are detected is to remove the locus in question, as was done here for one locus in samples from 2018.

For the selection of the response variable, we encourage using QI for studies investigating eoDNA quality and degradation that follow the "multi-tube" approach (Miquel et al., 2006; Taberlet et al., 1996). QI captures eoDNA degradation in greater detail than PCR success rate or genotyping errors alone by combining both information into one metric. This becomes most apparent toward higher values where QI differentiates between samples with 100% amplification success by leveraging genotyping errors as disagreement between replicates and consensus genotype (Appendix S1: Figure Supp_11 1, Supp_20 6).

While originally developed for microsatellites, QI can similarly be calculated for SNP loci. For presence/absence estimates from direct environmental samples like soil, air, or water (eDNA), a similar measure to QI has been developed and coined "eDNA score" (Biggs et al., 2015). However, Biggs et al. (2015) observed a low correlation between abundance estimates and "eDNA score" when abundance was high. Alternatively, one could quantify eDNA concentrations directly with qPCR while simultaneously performing classical abundance estimates (counting/trapping) and monitoring environmental conditions, to determine how environmental factors reduce eDNA concentration (Buxton et al., 2017). Another approach is monitoring decreasing eDNA concentration after removal of a known organism

abundance in various environmental treatments over time as seen in Strickler et al. (2015). Environmentally degraded eDNA concentration can then be expressed as proportion of such initial "undegraded" eDNA concentration and directly used as a binomial response variable in our pipeline. This has the advantage that eDNA concentration sampled in the field can be "back-translated" into initial "undegraded" eDNA concentration. With the best predictive model of Step 5, built with environmental treatment data and fed with environmental variables from the field, one could predict this proportion. Lastly, one simply divides sampled eDNA concentration by this predicted proportion to get eDNA concentration before environmental degradation, and therefrom estimates abundance or mass.

In conclusion, our pipeline can be applied across systems, eoDNA sources and study goals in existing and new datasets, ultimately improving sampling efficiency and accuracy of information gained from genetic material left behind by organisms in their environment.

CONFLICT OF INTEREST STATEMENT

The authors declare no conflict of interest.

DATA AVAILABILITY STATEMENT

The dataset including the pipeline to create the analyses presented in this publication are available on Dryad: https://doi.org/10.5061/dryad.79cnp5hxn.

BENEFIT-SHARING STATEMENT

Sample collection was approved by local authorities (permit number Jena AV09_AGO7_17).

ORCID

Thomas Naef https://orcid.org/0000-0001-8558-3927
Lisa Lehnen https://orcid.org/0000-0002-2481-7344
Eric J. Petit https://orcid.org/0000-0001-5058-5826
Jaap van Schaik https://orcid.org/0000-0003-4825-7676
Sebastien J. Puechmaille https://orcid.org/0000-0001-9517-5775

REFERENCES

Abdel-Gany, S. S., El-Badry, M. O., Fahmy, A. S., & Mohamed, S. A. (2017). Purification and characterization of deoxyribonuclease from small intestine of camel *Camelus dromedarius*. *Journal of Genetic Engineering and Biotechnology*, 15, 463–467. https://doi.org/10.1016/j.jgeb.2017.06.008

Agetsuma-Yanagihara, Y., Inoue, E., & Agetsuma, N. (2017). Effects of time and environmental conditions on the quality of DNA extracted from fecal samples for genotyping of wild deer in a warm temperate broad-leaved forest. *Mammal Research*, 62, 201–207. https://doi.org/10.1007/s13364-016-0305-x

Biggs, J., Ewald, N., Valentini, A., Gaboriaud, C., Dejean, T., Griffiths, R. A., Foster, J., Wilkinson, J. W., Arnell, A., Brotherton, P., Williams, P., & Dunn, F. (2015). Using eDNA to develop a national citizen science-based monitoring programme for the great crested newt (*Triturus cristatus*). *Biological Conservation*, 183, 19–28. https://doi.org/10.1016/j.biocon.2014.11.029

Brooks, M. E., Kristensen, K., Benthem, K. J. V., Magnusson, A., Berg, C. W., Nielsen, A., Skaug, H. J., Mächler, M., & Bolker, B. M. (2017). glmmTMB balances speed and flexibility among packages for zero-inflated generalized linear mixed modeling. *The R Journal*, 9, 378–400. https://doi.org/10.32614/rj-2017-066

Broquet, T., Ménard, N., & Petit, E. (2006). Noninvasive population genetics: A review of sample source, diet, fragment length and microsatellite motif effects on amplification success and genotyping error rates. *Conservation Genetics*, 8, 249–260. https://doi.org/10.1007/s10592-006-9146-5

Buxton, A. S., Groombridge, J. J., Zakaria, N. B., & Griffiths, R. A. (2017). Seasonal variation in environmental DNA in relation to population size and environmental factors. *Scientific Reports*, 7, 46294. https://doi.org/10.1038/srep46294

Cade, B. S. (2015). Model averaging and muddled multimodel inferences. *Ecology*, 96, 2370–2382. https://doi.org/10.1890/14-1639.1

Dash, H. R., & Das, S. (2018). Microbial degradation of forensic samples of biological origin: Potential threat to human DNA typing. *Molecular Biotechnology*, 60, 141–153. https://doi.org/10.1007/s12033-017-0052-5

Dormann, C. F., Elith, J., Bacher, S., Buchmann, C., Carl, G., Carré, G., Marquéz, J. R. G., Gruber, B., Lafourcade, B., Leitão, P. J., Münkemüller, T., McClean, C., Osborne, P. E., Reineking, B., Schröder, B., Skidmore, A. K., Zurell, D., & Lautenbach, S. (2013). Collinearity: A review of methods to deal with it and a simulation study evaluating their performance. *Ecography*, 36, 27–46. https://doi.org/10.1111/j.1600-0587.2012.07348.x

Eichmiller, J. J., Best, S. E., & Sorensen, P. W. (2016). Effects of temperature and trophic state on degradation of environmental DNA in lake water. *Environmental Science & Technology*, 50, 1859–1867. https://doi.org/10.1021/acs.est.5b05672

Freckleton, R. P. (2010). Dealing with collinearity in behavioural and ecological data: Model averaging and the problems of measurement error. *Behavioral Ecology and Sociobiology*, 65, 91–101. https://doi.org/10.1007/s00265-010-1045-6

Gelman, A. (2008). Scaling regression inputs by dividing by two standard deviations. *Statistics in Medicine*, 27, 2865–2873. https://doi.org/10.1002/sim.3107

Grueber, C. E., Nakagawa, S., Laws, R. J., & Jamieson, I. G. (2011). Multimodel inference in ecology and evolution: Challenges and solutions. *Journal of Evolutionary Biology*, 24, 699–711. https://doi.org/10.1111/j.1420-9101.2010.02210.x

Harrell, F. E. J., & Charles, D. (2021). *Hmisc: Harrell miscellaneous*. Package version 4.5-0. https://CRAN.R-project.org/package=Hmisc

Harrison, X. A. (2015). A comparison of observation-level random effect and beta-binomial models for modelling overdispersion in binomial data in ecology & evolution. *PeerJ*, 3, e1114. https://doi.org/10.7717/peerj.1114

Harrison, X. A., Donaldson, L., Correa-Cano, M. E., Evans, J., Fisher, D. N., Goodwin, C. E. D., Robinson, B. S., Hodgson, D. J., & Inger, R. (2018). A brief introduction to mixed effects modelling and multi-model inference in ecology. *PeerJ*, 6, e4794. https://doi.org/10.7717/peerj.4794

Hartig, F. (2021). *DHARMa: Residual diagnostics for hierarchical (multilevel/mixed) regression models*. R package version 0.4.2. http://florianhartig.github.io/DHARMa/

Hothorn, T., Bretz, F., & Westfall, P. (2008). Simultaneous inference in general parametric models. *Biometrical Journal*, 50, 346–363. https://doi.org/10.1002/bimj.200810425

James, G., Witten, D., Hastie, T., & Tibshirani, R. (2021). *An introduction to statistical learning* (2nd ed.). Springer US.

Jan, P. L., Lehnen, L., Besnard, A. L., Kerth, G., Biedermann, M., Schorcht, W., Petit, E. J., Le Gouar, P., & Puechmaille, S. J. (2019). Range expansion is associated with increased survival and fecundity in a long-lived bat species. *Proceedings of the Royal Society B: Biological Sciences*, 286, 20190384. https://doi.org/10.1098/rspb.2019.0384

Lefort, M.-C., Cruickshank, R. H., Descovich, K., Adams, N. J., Barun, A., Emami-Khoyi, A., Ridden, J., Smith, V. R., Sprague, R., Waterhouse, B., & Boyer, S. (2022). Blood, sweat and tears: A review of non-invasive DNA sampling. *Peer Community Journal*, 2. https://doi.org/10.24072/pcjournal.98

Lehnen, L., Jan, P. L., Besnard, A. L., Fourcy, D., Kerth, G., Biedermann, M., Nyssen, P., Schorcht, W., Petit, E. J., & Puechmaille, S. J. (2021). Genetic diversity in a long-lived mammal is explained by the past's demographic shadow and current connectivity. *Molecular Ecology*, 30, 5048–5063. https://doi.org/10.1111/mec.16123

Lehnen, L., Schorcht, W., Karst, I., Biedermann, M., Kerth, G., & Puechmaille, S. J. (2018). Using approximate Bayesian computation to infer sex ratios from acoustic data. *PLoS One*, 13, e0199428. https://doi.org/10.1371/journal.pone.0199428

Lüdecke, D. (2018). ggeffects: Tidy data frames of marginal effects from regression models. *Journal of Open Source Software*, 3, 772. https://doi.org/10.21105/joss.00772

Lüdecke, D., Makowski, D., Waggoner, P., & Patil, I. (2020). *Performance: Assessment of regression models performance*. CRAN. https://doi.org/10.5281/zenodo.3952174

Lugg, W. H., Griffiths, J., Rooyen, A. R., Weeks, A. R., Tingley, R., & Jarman, S. (2017). Optimal survey designs for environmental DNA sampling. *Methods in Ecology and Evolution*, 9, 1049–1059. https://doi.org/10.1111/2041-210x.12951

Mäck, K., Scharbert, A., Schulz, R., & Sahm, R. (2021). A new approach combining forensic thresholds and a multiple-tubes approach to unravel false microsatellite profiles from cross-contaminated sample material. *Conservation Genetics Resources*, 13, 89–95. https://doi.org/10.1007/s12686-020-01175-3

Marshall, N. T., Vanderploeg, H. A., & Chaganti, S. R. (2021). Environmental (e)RNA advances the reliability of eDNA by predicting its age. *Scientific Reports*, 11, 2769. https://doi.org/10.1038/s41598-021-82205-4

Maxim Integrated Products, I. (2015). *DS1923 iButton Hygrochron Temperature/Humidity Logger with 8KB Datalog Memory*. https://datasheets.maximintegrated.com/en/ds/DS1923.pdf

Miquel, C., Bellemain, E., Poillot, C., Bessière, J., Durand, A., & Taberlet, P. (2006). Quality indexes to assess the reliability of genotypes in studies using noninvasive sampling and multiple-tube approach. *Molecular Ecology Notes*, 6, 985–988. https://doi.org/10.1111/j.1471-8286.2006.01413.x

Murphy, M. A., Kendall, K. C., Robinson, A., & Waits, L. P. (2007). The impact of time and field conditions on brown bear (*Ursus arctos*) faecal DNA amplification. *Conservation Genetics*, 8, 1219–1224. https://doi.org/10.1007/s10592-006-9264-0

Naef, T., Besnard, A. L., Lehnen, L., Petit, E., van Schaik, J., & Puechmaille, S. J. (2023). How to quantify factors degrading DNA in the environment and predict degradation for effective sampling design. https://doi.org/10.5061/dryad.79cnp5hxn

Nsubuga, A. M., Robbins, M. M., Roeder, A. D., Morin, P. A., Boesch, C., & Vigilant, L. (2004). Factors affecting the amount of genomic DNA extracted from ape faeces and the identification of an improved sample storage method. *Molecular Ecology*, 13, 2089–2094. https://doi.org/10.1111/j.1365-294X.2004.02207.x

Puechmaille, S. J., Mathy, G., & Petit, E. J. (2007). Good DNA from bat droppings. *Acta Chiropterologica*, 9, 269–276. https://doi.org/10.3161/1733-5329(2007)9[269:GDFBD]2.0.CO;2

Puechmaille, S. J., & Petit, E. J. (2007). Empirical evaluation of non-invasive capture-mark-recapture estimation of population size based on a single sampling session. *Journal of Applied Ecology*, 44, 843–852. https://doi.org/10.1111/j.1365-2664.2007.01321.x

R Core Team. (2021). *R: A language and environment for statistical computing*. https://www.R-project.org/

Rees, H. C., Maddison, B. C., Middleditch, D. J., Patmore, J. R. M., Gough, K. C., & Crispo, E. (2014). The detection of aquatic animal species using environmental DNA – A review of eDNA as a survey tool in ecology. *Journal of Applied Ecology*, 51, 1450–1459. https://doi.org/10.1111/1365-2664.12306

Regnaut, S., Lucas, F. S., & Fumagalli, L. (2005). DNA degradation in avian faecal samples and feasibility of non-invasive genetic studies of threatened capercaillie populations. *Conservation Genetics*, 7, 449–453. https://doi.org/10.1007/s10592-005-9023-7

Richards, S. A. (2007). Dealing with overdispersed count data in applied ecology. *Journal of Applied Ecology*, 45, 218–227. https://doi.org/10.1111/j.1365-2664.2007.01377.x

Roberts, D. R., Bahn, V., Ciuti, S., Boyce, M. S., Elith, J., Guillera-Arroita, G., Hauenstein, S., Lahoz-Monfort, J. J., Schröder, B., Thuiller, W., Warton, D. I., Wintle, B. A., Hartig, F., & Dormann, C. F. (2017). Cross-validation strategies for data with temporal, spatial, hierarchical, or phylogenetic structure. *Ecography*, 40, 913–929. https://doi.org/10.1111/ecog.02881

Rodriguez-Ezpeleta, N., Morissette, O., Bean, C. W., Manu, S., Banerjee, P., Lacoursiere-Roussel, A., Beng, K. C., Alter, S. E., Roger, F., Holman, L. E., Stewart, K. A., Monaghan, M. T., Mauvisseau, Q., Mirimin, L., Wangensteen, O. S., Antognazza, C. M., Helyar, S. J., de Boer, H., Monchamp, M. E., … Deiner, K. (2021). Trade-offs between reducing complex terminology and producing accurate interpretations from environmental DNA: Comment on "Environmental DNA: What's behind the term?" by Pawlowski et al., (2020). *Molecular Ecology*, 30, 4601–4605. https://doi.org/10.1111/mec.15942

RStudio Team. (2021). *RStudio: Integrated development environment for R*. http://www.rstudio.com/

Santini, A., Lucchini, V., Fabbri, E., & Randi, E. (2007). Ageing and environmental factors affect PCR success in wolf (*Canis lupus*) excremental DNA samples. *Molecular Ecology Notes*, 7, 955–961. https://doi.org/10.1111/j.1471-8286.2007.01829.x

Sawaya, M. A., Seitz, T., & Stetz, J. B. (2015). Effects of exposure on genotyping success rates of hair samples from brown and American black bears. *Journal of Fish and Wildlife Management*, 6, 191–198. https://doi.org/10.3996/122013-jfwm-085

Schielzeth, H. (2010). Simple means to improve the interpretability of regression coefficients. *Methods in Ecology and Evolution*, 1, 103–113. https://doi.org/10.1111/j.2041-210X.2010.00012.x

416 | **WILEY**—Environmental DNA
Open Access
Dedicated to the study and use of environmental DNA for basic and applied sciences

NAEF ET AL.

Schielzeth, H., Dingemanse, N. J., Nakagawa, S., Westneat, D. F., Allegue, H., Teplitsky, C., Réale, D., Dochtermann, N. A., Garamszegi, L. Z., Araya-Ajoy, Y. G., & Sutherland, C. (2020). Robustness of linear mixed-effects models to violations of distributional assumptions. *Methods in Ecology and Evolution*, *11*, 1141–1152. https://doi.org/10.1111/2041-210x.13434

Strickler, K. M., Fremier, A. K., & Goldberg, C. S. (2015). Quantifying effects of UV-B, temperature, and pH on eDNA degradation in aquatic microcosms. *Biological Conservation*, *183*, 85–92. https://doi.org/10.1016/j.biocon.2014.11.038

Taberlet, P., Griffin, S., Goossens, B., Questiau, S., Manceau, V., Escaravage, N., Waits, L. P., & Bouvet, J. (1996). Reliable genotyping of samples with very low DNA quantities using PCR. *Nucleic Acids Research*, *24*, 3189–3194. https://doi.org/10.1093/nar/24.16.3189

Taberlet, P., Waits, L. P., & Luikart, G. (1999). Noninvasive genetic sampling: Look before you leap. *Trends in Ecology & Evolution*, *14*, 323–327. https://doi.org/10.1016/s0169-5347(99)01637-7

Thomsen, P. F., & Willerslev, E. (2015). Environmental DNA – An emerging tool in conservation for monitoring past and present biodiversity. *Biological Conservation*, *183*, 4–18. https://doi.org/10.1016/j.biocon.2014.11.019

Vili, N., Nemesházi, E., Kovács, S., Horváth, M., Kalmár, L., & Szabó, K. (2013). Factors affecting DNA quality in feathers used for non-invasive sampling. *Journal of Ornithology*, *154*, 587–595. https://doi.org/10.1007/s10336-013-0932-9

Walker, F. M., Tobin, A., Simmons, N. B., Sobek, C. J., Sanchez, D. E., Chambers, C. L., & Fofanov, V. Y. (2019). A fecal sequel: Testing the limits of a genetic assay for bat species identification. *PLoS One*, *14*, e0224969. https://doi.org/10.1371/journal.pone.0224969

Wasser, S. K., Houston, C. S., Koehler, G. M., Cadd, G. G., & Fain, S. R. (1997). Techniques for application of faecal DNA methods to field studies of Ursids. *Molecular Ecology*, *6*, 1091–1097. https://doi.org/10.1046/j.1365-294x.1997.00281.x

Zarzoso-Lacoste, D., Jan, P.-L. L., Lehnen, L., Girard, T., Besnard, A.-L. L., Puechmaille, S. J., & Petit, E. J. (2018). Combining noninvasive genetics and a new mammalian sex-linked marker provides new tools to investigate population size, structure and individual behaviour: An application to bats. *Molecular Ecology Resources*, *18*, 217–228. https://doi.org/10.1111/1755-0998.12727

Zarzoso-Lacoste, D., Jan, P.-L. L., Lehnen, L., Girard, T., Besnard, A.-L. L., Puechmaille, S. J., & Petit, E. J. (2020). Corrigendum. *Molecular Ecology Resources*, *20*, 1787. https://doi.org/10.1111/1755-0998.13254

Zuur, A. F., Ieno, E. N., & Freckleton, R. (2016). A protocol for conducting and presenting results of regression-type analyses. *Methods in Ecology and Evolution*, *7*, 636–645. https://doi.org/10.1111/2041-210x.12577

SUPPORTING INFORMATION

Additional supporting information can be found online in the Supporting Information section at the end of this article.

How to cite this article: Naef, T., Besnard, A.-L., Lehnen, L., Petit, E. J., van Schaik, J., & Puechmaille, S. J. (2023). How to quantify factors degrading DNA in the environment and predict degradation for effective sampling design. *Environmental DNA*, *5*, 403–416. https://doi.org/10.1002/edn3.414